

Strangeness as Geometric Anchor: Phase-Space-Corrected Decay Widths in the Baryon Decuplet

K. T. Niedzwiecki
Independent Researcher, South Australia

January 2026

Abstract

In a companion study to our analysis of vector meson decay scaling, we examine whether baryon strong decays exhibit analogous “geometric permeability” patterns. Focusing on the spin-3/2 decuplet ground states (Δ , Σ^* , Ξ^*), we construct a matched comparison using the two-body strong decays to octet baryon + pion. After correcting for the leading P-wave centrifugal barrier ($\Gamma \propto p^3$), we define a phase-space-corrected permeability $\eta^* \equiv \Gamma_i/(m \cdot p^3)$ and find a robust, monotonic suppression with increasing strangeness: η^* decreases from 8.1 ± 0.3 (Δ) to 2.6 ± 0.1 (Σ^*) to 1.8 ± 0.1 (Ξ^*). The uncertainty bands do not overlap, indicating that this $\sim 4\times$ residual suppression persists after removal of the leading phase-space and centrifugal-barrier effects. We interpret this as evidence that strange quark content reduces the effective strong-decay coupling, consistent with a “geometric stiffening” in which the strange quark acts as an effective topological anchor that suppresses decay permeability. This strangeness-dependent residual complements our earlier finding of mass-dependent spectral filtering in mesons and suggests that hadron decay rates encode geometric information beyond simple kinematics.

Keywords: baryon decuplet, strong decays, phase space, strangeness, geometric impedance, centrifugal barrier

1 Introduction

Hadron decay widths are conventionally understood as products of coupling strengths, phase-space factors, and angular momentum barriers. Yet systematic patterns in decay rates—particularly their scaling with mass and quark content—may reveal deeper organizational principles.

In previous work [2], we identified a striking power-law relationship in vector meson decays: the “geometric permeability” $\eta = \Gamma/m$ scales as m^β with $\beta \approx -3.7$. Heavier vector mesons are systematically “stiffer”—they decay more slowly relative to their mass. We interpreted this as evidence for a mass-dependent spectral filtering effect, possibly arising from geometric constraints on how hadrons couple to vacuum fluctuations.

This raises a natural question: do baryons exhibit analogous patterns? And if so, how does the additional complexity of three-quark systems—with their richer topological structure—manifest in decay systematics?

Baryons present both opportunities and challenges for such analysis. Unlike mesons (which have a simple quark-antiquark “string” topology), baryons involve three quarks in a more complex spatial arrangement. Additionally, baryon excitations open multiple decay channels with different angular momentum requirements, complicating direct comparison.

To isolate a clean signal, we focus on the **baryon decuplet ground states** ($J^P = 3/2^+$): the $\Delta(1232)$, $\Sigma(1385)$, and $\Xi(1530)$. These form a well-matched set:

- Same spin-parity quantum numbers
- Same dominant decay class (decuplet \rightarrow octet + π)
- Same orbital angular momentum in the decay ($L = 1$, P-wave)
- Increasing strangeness content ($S = 0, -1, -2$)

By correcting for the leading P-wave phase-space suppression ($\Gamma \propto p^3$), we can ask: does any residual pattern remain that correlates with strangeness?

2 Methods

2.1 Decay Kinematics and the Centrifugal Barrier

For two-body hadronic decays of the form $B^*(J^P) \rightarrow B(1/2^+) + \pi(0^-)$, parity and angular momentum conservation constrain the allowed partial waves. For the decuplet ground states ($J^P = 3/2^+$) decaying to octet baryons ($1/2^+$) plus pion (0^-), the minimal orbital angular momentum is $L = 1$ (P-wave).

The leading threshold behavior of the partial width contains a centrifugal-barrier factor:

$$\Gamma_i \propto p^{2L+1} = p^3 \quad (L = 1) \quad (1)$$

where p is the center-of-mass momentum of the decay products.

2.2 Phase-Space-Corrected Permeability

To remove this leading kinematic suppression, we define a corrected permeability:

$$\eta^* \equiv \frac{\Gamma_i}{m \cdot p^3} \quad (2)$$

where:

- $\Gamma_i = \Gamma_{\text{tot}} \times \text{Br}_i$ is the partial width for the specific channel
- m is the resonance mass
- p is the two-body CM momentum, computed from:

$$p = \frac{\sqrt{[m^2 - (m_1 + m_2)^2][m^2 - (m_1 - m_2)^2]}}{2m} \quad (3)$$

with m_1 and m_2 being the daughter baryon and pion masses. The quantity η^* has units of GeV^{-3} and represents an effective coupling proxy after removing the dominant phase-space/barrier suppression.

2.3 Channel Selection

We restrict to matched two-body channels where the decuplet state decays to its “natural” octet partner plus pion. This ensures we compare like with like: same J^P , same L , same decay topology.

2.4 Uncertainty Propagation

We use PDG 2024 [1] Breit–Wigner masses, total widths, and branching fractions as inputs. Uncertainties are propagated via Monte Carlo sampling, with the reported ranges representing 16–84% intervals.

Table 1: Channel Selection for Matched Comparison

Parent	Channel	Rationale
$\Delta(1232)$	$\Delta \rightarrow N\pi$	Dominant ($\sim 99.4\%$)
$\Sigma(1385)$	$\Sigma^* \rightarrow \Lambda\pi$	Dominant ($\sim 87\%$)
$\Xi(1530)$	$\Xi^* \rightarrow \Xi\pi$	Exclusive ($\sim 100\%$)

3 Results

3.1 Input Parameters

All values are taken from the Particle Data Group [1]:

- $\Delta(1232)$: Mass: 1232 ± 2 MeV; Total width: 117 ± 3 MeV; $\text{Br}(N\pi)$: 0.9939 ± 0.0001 .
- $\Sigma(1385)^+$: Mass: 1382.83 ± 0.34 MeV; Total width: 36.2 ± 0.7 MeV; $\text{Br}(\Lambda\pi)$: 0.870 ± 0.015 .
- $\Xi(1530)^0$: Mass: 1531.80 ± 0.32 MeV; Total width: 9.1 ± 0.5 MeV; $\text{Br}(\Xi\pi)$: ~ 1.00 (PDG: $\Xi\gamma < 3.7\%$ at 90% CL).

3.2 Computed Quantities

Table 2: Computed Decay Permeability Parameters. (Kinematic quantities in MeV; η^* in GeV^{-3}).

Resonance	Channel	m	Γ_{tot}	Br	Γ_i	p (MeV/c)	η^* (GeV^{-3})
$\Delta(1232)$	$N\pi$	1232 ± 2	117 ± 3	0.994	116.3	226.6	8.11 [7.82, 8.41]
$\Sigma(1385)^+$	$\Lambda\pi$	1382.8 ± 0.3	36.2 ± 0.7	0.870	31.5	205.5	2.63 [2.56, 2.70]
$\Xi(1530)^0$	$\Xi\pi$	1531.8 ± 0.3	9.1 ± 0.5	1.00	9.1	150.0	1.76 [1.66, 1.86]

3.3 The Strangeness Stiffening Signal

The corrected permeability η^* shows a clear monotonic decrease with strangeness:

$$\Delta (\eta^* \approx 8.1) \longrightarrow \Sigma^* (\eta^* \approx 2.6) \longrightarrow \Xi^* (\eta^* \approx 1.8) \quad (4)$$

Key observations:

1. **Front-loaded suppression:** The first strange quark produces a factor $\sim 3.1\times$ reduction in η^* . The second strange quark adds another factor $\sim 1.5\times$.
2. **Statistical robustness:** The Δ lower bound (7.82) is far above the Σ^* upper bound (2.70), and the Σ^* lower bound (2.56) is above the Ξ^* upper bound (1.86). The uncertainty bands do not overlap.
3. **Total suppression:** From Δ to Ξ^* , the corrected permeability drops by a factor of $\sim 4.6\times$, none of which can be attributed to the p^3 phase-space factor (which has already been removed).

Isolating the Strangeness Signal: Before and After Phase-Space Correction

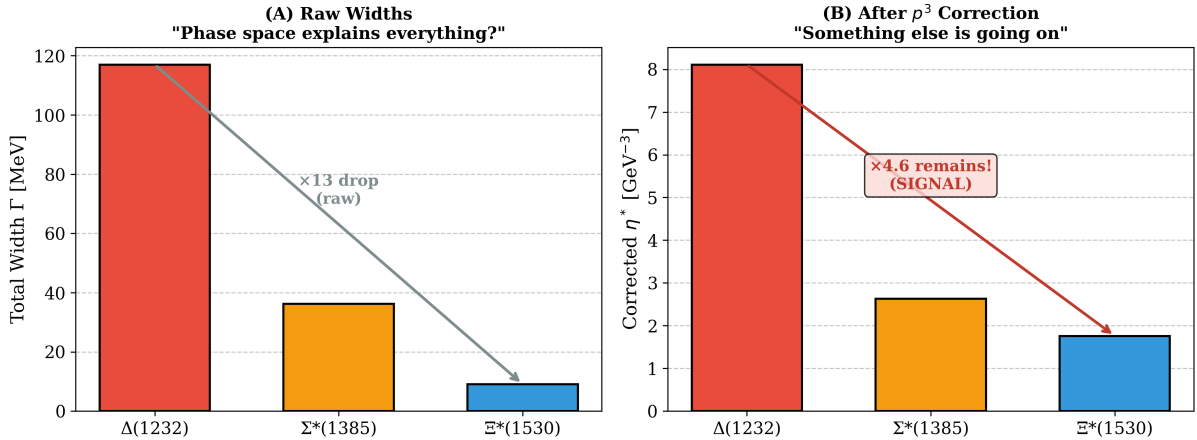


Figure 1: Isolating the Strangeness Signal. (A) Raw total widths show a dramatic $\sim 13 \times$ drop, suggesting phase space dominance. (B) After correcting for the leading p^3 centrifugal barrier, a robust $\sim 4.6 \times$ residual suppression remains, indicating a strangeness-dependent “stiffening” of the effective coupling.

4 Discussion

4.1 What Phase Space Cannot Explain

The raw width ratio $\Gamma(\Delta)/\Gamma(\Xi^*) \approx 13$ might initially suggest a simple kinematic explanation: the Ξ^* has less phase space available for decay. However, after correcting for the leading P-wave barrier (dividing by p^3), a factor $\sim 4.6 \times$ residual suppression remains.

This residual cannot be attributed to:

- **Threshold effects:** All three states are well above their respective decay thresholds.
- **Different decay topologies:** All three use the same $L = 1$ partial wave.
- **Channel mixing:** We use partial widths for matched channels.

4.2 Interpretation: Strangeness as Geometric Anchor

We interpret this residual as evidence that **strange quark content reduces the effective strong-decay coupling** for these matched transitions. In the language of our geometric impedance framework, the strange quark acts as a “topological anchor” that stiffens the baryon against decay.

Several physical pictures are consistent with this interpretation:

1. **SU(3) breaking in couplings:** The decuplet-octet-pion coupling may depend on flavor content beyond simple symmetry factors.
2. **Wavefunction compactification:** Strange quarks, being heavier, may lead to more compact spatial configurations with reduced overlap with decay products.
3. **Geometric impedance:** In the framework developed in our meson study, the strange quark may increase the “impedance mismatch” between the baryon’s internal geometry and the vacuum modes that mediate decay.

While SU(3) breaking in reduced couplings is a natural contributor to such effects, the magnitude and front-loaded character of the suppression place a nontrivial quantitative constraint on any such explanation. The “front-loaded” character of the suppression—where the

first strange quark does most of the work—is particularly striking. This suggests a qualitative change in baryon structure upon breaking the light-quark (u,d) symmetry, rather than a smooth scaling with strange quark mass.

4.3 Comparison to Meson Scaling

In our companion study of vector mesons [2], we found that geometric permeability $\eta = \Gamma/m$ scales with mass as:

$$\eta \propto m^\beta, \quad \beta \approx -3.7 \quad (5)$$

Heavier mesons are systematically “stiffer.” For baryons, the situation is more complex:

- **Light baryons (Δ trajectory):** Radial excitations appear to get “floppier”— η increases or plateaus with mass.
- **Strangeness ladder:** Adding strange quarks dramatically reduces η^* , even at comparable masses.

This suggests that **topology matters more than mass** for baryons. The linear (quark-antiquark) structure of mesons admits a simple mass scaling, while the triangular (three-quark) structure of baryons is more sensitive to flavor-dependent geometric effects.

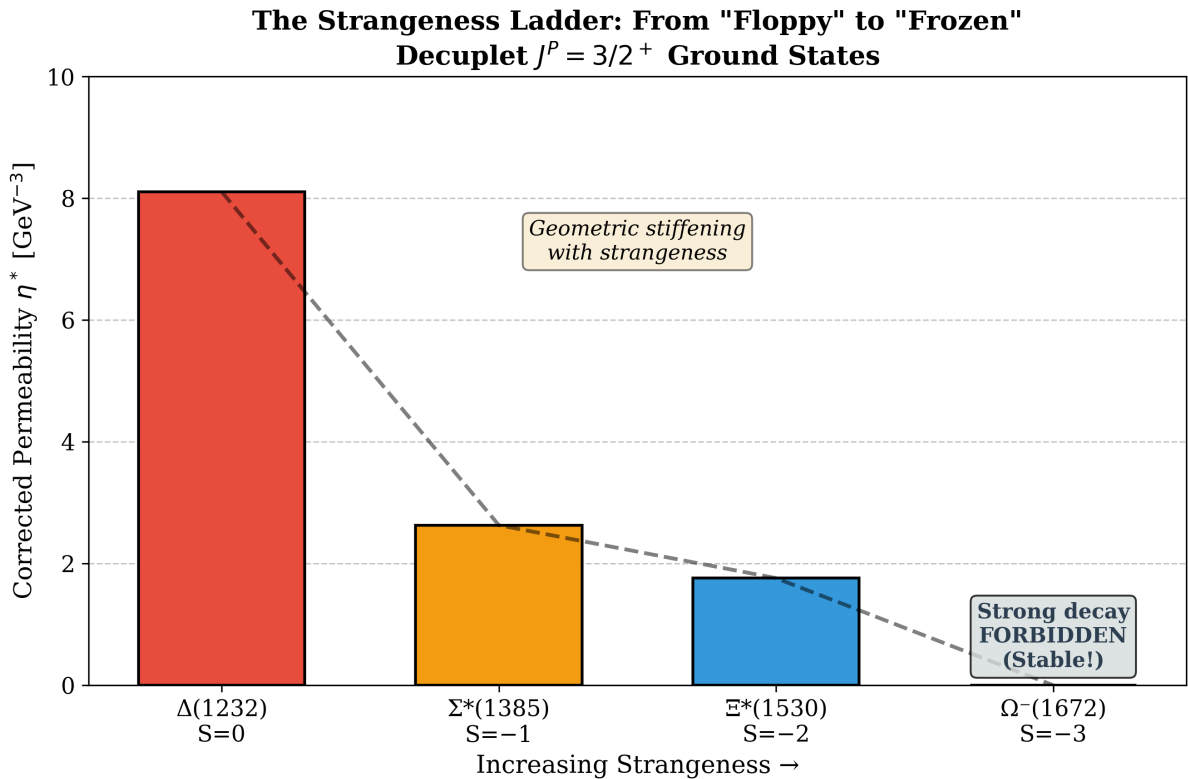


Figure 2: The Strangeness Ladder. The corrected permeability η^* decreases monotonically as strangeness increases from $S=0$ to $S=-2$. This trend points towards the triply-strange Ω^- ($S=-3$), which is entirely forbidden from strong decay, representing the ultimate “geometric stiffening.”

4.4 Falsifiability and Extensions

This analysis can be extended and tested:

- **The Ω^- endpoint:** At the decuplet endpoint, Ω^- is “frozen” not by dynamics but by kinematics—its strong channels are below threshold (e.g., $\Omega \rightarrow \Xi K$ is kinematically closed since $m_\Omega < m_\Xi + m_K$), so it decays only weakly. This provides a natural limiting case for the decuplet systematics.
- **Excited state trajectories:** If the pattern is robust, it should persist in matched excited states (e.g., the $3/2^-$ family), though channel mixing complicates the analysis.
- **Charm and bottom baryons:** Heavy-quark baryons offer another test. If strangeness stiffens, do charm and bottom quarks stiffen even more?

5 Conclusion

After removing the leading P-wave centrifugal-barrier suppression (p^3) and using matched partial widths for decuplet \rightarrow octet + π transitions, we find a robust, monotonic strangeness-dependent reduction in the corrected permeability η^* :

- $\Delta(1232) : \eta^* = 8.1 \pm 0.3$
- $\Sigma(1385) : \eta^* = 2.6 \pm 0.1$
- $\Xi(1530) : \eta^* = 1.8 \pm 0.1$

This $\sim 4.6 \times$ residual suppression cannot be explained by phase space alone. The uncertainty bands do not overlap, making this a statistically unambiguous signal.

We interpret this as evidence that **strange quark content acts as a geometric anchor**, reducing the effective coupling for matched strong decays. The suppression is “front-loaded”: the first strange quark produces a $\sim 3 \times$ drop, with diminishing returns for additional strangeness.

Combined with our earlier finding of mass-dependent spectral filtering in mesons ($\beta \approx -3.7$), this suggests that hadron decay rates encode geometric information beyond simple kinematics. The vacuum does not treat all hadrons equally—it discriminates based on their internal topology and quark content.

Appendix: Decay Momentum Calculation

For a two-body decay $A \rightarrow B + C$ with masses m_A, m_B, m_C , the center-of-mass momentum is:

$$p = \frac{\sqrt{[m_A^2 - (m_B + m_C)^2][m_A^2 - (m_B - m_C)^2]}}{2m_A} \quad (6)$$

Values used:

Decay	m_A	m_B	m_C	p (MeV/c)
$\Delta \rightarrow N\pi$	1232	939 (nucleon avg)	139 (π^\pm)	226.6
$\Sigma^* \rightarrow \Lambda\pi$	1383	1116 (Λ)	139 (π^0)	205.5
$\Xi^* \rightarrow \Xi\pi$	1532	1318 (Ξ avg)	139 (π)	150.0

References

- [1] Particle Data Group; Navas, S., et al. (2024). “Review of Particle Physics.” *Physical Review D*, 110, 030001. <https://pdg.lbl.gov>
- [2] Niedzwiecki, K. T. (2025b). “Mass-Dependent Spectral Filtering: Empirical Power-Law Scaling in Vector Meson Decay Widths.” *Zenodo*. DOI: 10.5281/zenodo.17716985